




# A geospatial assessment of flood hazard in north-eastern depressed basin, Bangladesh

Mohammad Abdul Quader,<sup>1</sup>  Hemal Dey,<sup>1,2</sup> Md. Abdul Malak<sup>1,3</sup> and Md. Zakiur Rahman<sup>4,5</sup>

<sup>1</sup>Department of Geography and Environment, Jagannath University, Dhaka, Bangladesh

<sup>2</sup>Department of Geography, The University of Alabama, Tuscaloosa, Alabama, USA

<sup>3</sup>School of Geography and Sustainable Communities, University of Wollongong, NSW, Australia

<sup>4</sup>Department of Geography and Environmental Science, Begum Rokeya University, Rangpur, Bangladesh

<sup>5</sup>Department of Urban and Regional Planning and Geo-Information Management, Faculty of Geo-Information Science and Earth Observation, University of Twente, The Netherlands

Correspondence: Mohammad Abdul Quader (email: [quader@geography.jnu.ac.bd](mailto:quader@geography.jnu.ac.bd))

Floods are a frequently occurring calamity in deltaic Bangladesh. This paper aims to assess the temporal expansion of waterbodies during flooding using geospatial techniques. Several water indices were applied to classify the satellite images at various temporal scales. Among them, the Normalized Difference Water Index (NDWI) showed the highest correlation ( $r = 0.831$ ; where  $p = 0.01$ ) with rainfall data. Specifically, the NDWI results showed that perennial waterbodies measured 37 km<sup>2</sup> and 60 km<sup>2</sup> in Sunamganj District in 2017 and 2019, respectively. The area of waterbodies notably increased 52-fold from March to April (37 km<sup>2</sup> to 1958 km<sup>2</sup>) during the pre-monsoon flash flood of 2017. During the July 2019 monsoon flood, waterbodies started to extend after May and flooded 2784 km<sup>2</sup> in area. NDVI analysis showed that in 2019, floodwater submerged 361.7 km<sup>2</sup> of vegetation cover. At the same time, the Surma River's flooding resulted in a 73.9 per cent inundation of the total area of the Sunamganj District. We hope that this study will provide better understanding of the varying nature of floods that occur in the low lying bowl shaped Haor region which will in turn assist the government with flood mitigation.

**Keywords:** flash-floods, depressed basin, geospatial analysis, water extension, Haor topography, water levels

**Accepted:** 20 April 2022

## Introduction

Floods are the most devastating natural catastrophes in the world as they cause greater loss of lives and property damage when compared to any other natural phenomena (Jeyaseelan, 2004). With increasing population as well as anthropogenic impacts and climate change, floods have become more widespread and more problematic across the world (Malik *et al.*, 2020). In Bangladesh, the frequency and severity of flooding are increasing year upon year (Adnan *et al.*, 2020; Rayhan, 2010). Generally, 20.5 per cent of the country is being flooded every year (reaching up to 70 per cent in extreme scenarios) due to rainfall or the overflow of riverbanks, causing severe damage to the national economy (Benson & Clay, 2002; Mirza, 2002). In the north-eastern part of the country, there is a low-lying bowl-shaped depressed basin (locally known as *Haor*), where it is estimated that approximately 6000 km<sup>2</sup> of the Sylhet division and 25 000 km<sup>2</sup> in total are severely affected by early flash flooding almost annually (Humanitarian Response, 2017; Kamruzzaman & Shaw, 2018; Salauddin & Islam, 2011).

Floods can be divided into four categories in Bangladesh: (1) flash floods originating from hilly areas, (2) monsoon floods, (3) rain-fed floods, and (4) floods caused by

storm surges (Rahman *et al.*, 2007). In Bangladesh, pre-monsoon flash floods occur almost every year in some parts of the northeast Haor basin between March and May while riverine flooding occurs between June and September. The latter is also known as the monsoon flood (Roy *et al.*, 2019). During the pre-monsoon season (March–May), the north-eastern part of Bangladesh often experiences flash floods, a major natural hazard in that region and one that vastly affects lives, property, and croplands. Flash floods damage thousands of hectares (ha) of *boro* rice crops, considered a staple crop in the country (Ahmed *et al.*, 2017; Roy *et al.*, 2019; Hossain *et al.*, 2017; Humanitarian Response, 2017). Agricultural wages also sometimes decline during the flooding months in inundated districts (Banerjee, 2007). Thus, floods are not only an immediate threat to lives but to livelihoods and nutrition.

In 2017, the north-eastern depressed region of Bangladesh experienced severe flash flooding, which damaged almost 100 per cent of the crops (Das *et al.*, 2017; Baishakhy & Islam, 2018). Rapid flooding began in the north-eastern part of Bangladesh on 28 March 2017 due to heavy rains in Meghalaya, India (Aldhshan *et al.*, 2019). The heavy rainfalls in 2017 (9000 mm, as recorded by the BMD) broke all previous records and rapidly raised the surface water levels in various rivers both in north-eastern Bangladesh and neighbouring upstream hilly catchments within India (Meghalaya state). This led to a flash runoff from the hilly rivers that inundated a significant portion of the floodplains and wetlands including five districts of Haor region, namely Sunamganj, Netrokona, Moulvibazar, Brahmanbaria and Sylhet, affecting almost 1 million households and damaging rice crops worth nearly USD 450 million (Kamal *et al.*, 2018; Aldhshan *et al.*, 2019). Moreover, a total of 4 667 000 people (31 per cent of whom were located in the affected areas) were impacted, and ten people lost their lives in six districts (Habiganj, Kishoreganj, Moulvibazar, Netrokona, Sunamganj and Sylhet) in the north-eastern part of Bangladesh. Furthermore, 18 969 houses were either fully or partially destroyed resulting in the contamination of over 24 per cent of freshwater sources (tube wells, ponds, and lakes) in Sunamganj District alone (Humanitarian Response, 2017). The 2017 floods severely damaged crops within almost 1037 km<sup>2</sup> in Sunamganj District (which was the worst affected area) causing severe economic damage (Aldhshan *et al.*, 2019).

More recently, in July 2019, millions of people were displaced when devastating floods occurred in large parts of India, Nepal and Bangladesh (BBC News, 2019). Rain-swollen rivers in Bangladesh broke through several embankments and inundated dozens of villages, destroying thousands of homes and displacing 200 000 people. Furthermore, the flooding in Bangladesh exposed more than 4 000 000 people to the risk of food insecurity and various diseases (Al Jazeera, 2019). Heavy rainfall in the middle and at the end of July resulted in the occurrence of floods in the northern and north-eastern regions of Bangladesh whereby floodwater persisted from 1 to 3 days in the north-eastern districts (Sylhet, Sunamganj, Moulvibazar, Habiganj, and Netrokona) (Daily Star, 2019a). In Sunamganj District, almost 13 000 people were stranded in waterlogged areas due to floodwater (Daily Star, 2019b) and more than 66 000 homes were destroyed (Al Jazeera, 2019). According to the Daily Disaster Situation Report (Ministry of Disaster Management and Relief, 2019), a total of 18 lives were lost to the 2019 Bangladesh flood; among them, four people died in Chittagong and Bandarban District on 15 July and three people perished in Sirajganj and Sylhet District on that same day, while a further nine people died in several districts on 16 July 2019; and two people died on 17 July 2019.

It has been predicted that the estimated average cost of flood damage in the coastal parts of Bangladesh is likely to rise from \$1180 to \$2601 million in 25 years (Adnan *et al.*, 2020). Therefore, to mitigate the severity of flood impacts and to develop forecasting facilities as well as disaster preparedness, it is necessary to identify and assess areas that are prone to flooding as well as the duration of water extension (Kwak, 2017; Rahman *et al.*, 2007). Remote sensing techniques, especially the spectral index-based classification method, are tools with great potential as they can provide useful data for flood monitoring, flood damage assessment, investigation of water resources, flood extent mapping, flood hazard prediction assessment and water resources planning (Profeti & Macintosh, 1997; Tv & Kn, 2019; Psomiadis *et al.*, 2019; Haibo *et al.*, 2011; Aldhshan *et al.*, 2019). Despite Bangladesh facing frequent floods (almost every year), advanced studies on flood hazards using remote sensing techniques remain infrequent and inadequate in the study area. Several studies were found focusing on recent flood scenarios in Bangladesh; however, most of them either related to coastal flood vulnerability and impact assessment due to sea level rise (e.g., Karim & Mimura, 2008; Bhuiyan & Dutta, 2012; Hoque *et al.*, 2019; Adnan *et al.*, 2019; Adnan *et al.*, 2020) or to flood situations related to the megacities of Bangladesh (e.g., Dewan, 2013; Ahmed *et al.*, 2018). Only a few of them focused directly on flood hazards, in particular, flood hazards relating to the north-eastern depressed basin of Bangladesh (e.g., Ahmed *et al.*, 2017; Hossain *et al.*, 2017; Haque & Basak, 2017; Kamal *et al.*, 2018; Kamruzzaman & Shaw, 2018).

Utilizing geo-spatial techniques and MODIS data, Islam *et al.* (2010) depicted the spatio-temporal extension of inundation resulting from floods in 2004 and 2007 across the whole of Bangladesh. Moreover, Uddin *et al.* (2019) mapped the entire inundated area during the Bangladesh flash floods of 2017 using Sentinel-1 SAR data and then assessed its accuracy by comparing the results with Landsat 8 OLI data. Hoque *et al.* (2019) applied a spatial multi-criteria-integrated approach for mapping flood vulnerability in the coastal region of Bangladesh by using the Analytic Hierarchy Process. Among the very few works on flash floods of the north-eastern Haor region, a study by Kamal *et al.* (2018) used index-methods to analyse resilience to flash floods. By utilizing remote sensing techniques, Aldhshan *et al.* (2019) worked on flash-flood area mapping and detected damaged agricultural lands in eight sub-districts of Sunamganj District by using Sentinel-1 (S1) SAR images and Landsat-8 images. In addition, Hossain *et al.* (2017) worked on Tanguar Haor (located in Sunamganj District) and used the maximum likelihood method to assess the loss of cropland due to a flash flood that occurred in April 2017. Similarly, Ahmed *et al.* (2017) used Multi-temporal Landsat-8 OLI and MODIS data in their work on delineating both cultivated and damaged *boro* crops due to the flash flood in Haor region in Bangladesh; however, they failed to depict the monsoon flood scenario of Haor region and the gradual water extension process.

From the preceding literature, we argue that researchers have paid less attention to mapping and comparing temporal water extension during both flash and monsoon floods using geospatial techniques in the north-eastern depressed basin of Bangladesh. Moreover, previous studies have lacked in explaining topographical influences on frequent Haor flooding. Considering this research gap found regarding flood events in the low-lying north-eastern part of Bangladesh, this study aims to compare the flood-affected area and gradual expansion of waterbodies during two major flood occurrences (i.e. the flash flood of 2017 and the monsoon flood of 2019) and to investigate the topographical influences on Sunamganj Haor flooding using geospatial techniques.

Despite some limitations, we hope that our research will enable researchers and planners to better understand the Haor topography and its influences on gradual flood-water extension. More importantly, we would like the findings of this research to aid government policymakers (i.e. National Disaster Management Council, Bangladesh Haor and Wetland Development Board and Bangladesh Water Development Board), local authorities and non-government organizations in formulating appropriate flood risk mitigation plans by demarcating frequently flooded zones. Further, this paper also aims to contribute to the agricultural sector by detecting flood prone areas as well as flooding periods which will in turn inform pre-disaster, recovery and mitigation initiatives.

## Materials and methods

### Study area

Sunamganj District is located in north-eastern Bangladesh within the Sylhet Division, which is also in the downstream part of the Meghna river basin (Basher *et al.*, 2018). It is bounded by the hilly catchment of Meghalaya state (India) to the north, Sylhet District to the east, Netrokona District to the west, and Habiganj District to the south (Figure 1). The Sunamganj District comprises 11 sub-districts and 1 thana, 87 unions, 1581 mauzas, 2887 villages, 4 paurashavas, 36 wards and 139 mahallas (BBS, 2011a). According to the Bangladesh Bureau of Statistics (BBS, 2011a), the total population of

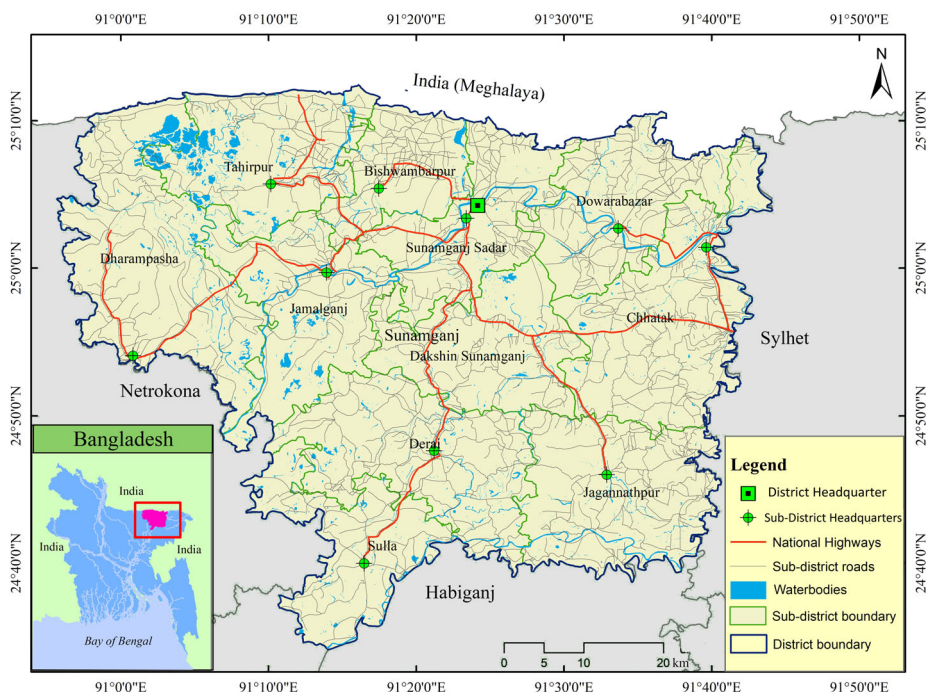


Figure 1. Map of the study area and location of Sunamganj District. The district headquarter (HQ), Sub-district HQ, national highway, and waterbodies are highlighted on the map. The inset map shows the location of the study area in Bangladesh.

Source: Figure produced by authors.

Sunamganj District (i.e. 2 467 968 inhabitants) live within an area of 3768.61km<sup>2</sup> with a population density of about 655 people per square kilometer and a literacy rate of 35 per cent. Its climate is cooler in the winter and warmer in the summer with heavy rainfall that occurs during the monsoon (BBS, 2011b). Sunamganj District's maximum and minimum temperature varies from 33.2°C to 13.6°C. Its annual average rainfall is 3334 mm (BBS, 2011a). The district—located in the country's northern, more elevated regions of the depression formation—has a young piedmont plain and a gentle sloping landscape mainly consisting of loamy sediments that may be subject to shallow flooding with coarser silt accretion behind existing embankments. In the middle, deeper part of that landscape, the soil contains blush silt clay of the old flood plain basin of the Surma and Kushiara rivers (BBS, 2011b). In between the milder slopes of the floodplain and the area where finer silts accreted, flooding occurred frequently during the monsoon season.

According to BBS (2011b) (Table 1), while the greatest proportion of highlands lies in the Bishwamvarpur sub-district (42 793 acres), a smaller area of highlands is found in Tahirpur sub-district (621 acres). Further, the greatest proportion of lowlands lies in the Dharampasha sub-district (68 546 acres). In terms of the number of waterbodies, Chhatak and Jagannath sub-districts have the largest number of ponds, i.e. 7060 and 4928, respectively. Of the 43 lakes in Sunamganj District, Bishwamvarpur sub-district has 40 lakes.

Figure 2 demonstrates water extension scenarios in the Tangua Haor area during the pre-monsoon season in 2018 (November 2018) and delineates the flooding in the Haor region in Sunamganj District. Image 01 shows (Hijol) trees partially submerged by the extension of perennial waters in the Haor region. Generally, this area is desiccated in the dry season. Farmers are used to cultivating several kinds of paddies over this area in the dry season. At the beginning of summer, the waterbodies started to extend, persisting till the late autumn season, flooding the areas depicted in Image 01. Image 02 shows people walking across the submerged roads to their homes. Seasonal flash floods regularly submerge several village roads. Image 03 shows a man collecting his cattle that graze on plants lying beneath the water. Image 04 reflects some

**Table 1. Land elevation, number of waterbodies and shelter centre information in the Sunamganj district.**

Sub-districts of Sunamganj	Land elevation (area in acres)			Waterbodies			Shelter centre	
	High land	Medium land	Low land	Ponds	Lakes	Rivers	Flood shelter	Cyclone shelter
Bishwamvarpur	42793	6014	12633	150	40	2	0	0
Chhatak	10883	27210	16536	7060	0	2	5	4
Dakshin Sunamganj	5805	71875	10573	160	0	1	0	0
Deraï	5412	14735	13432	20	0	3	0	0
Dharmapasha	4570	18278	68546	716	1	2	1	0
Doarabazar	3960	12885	5895	1850	0	1	0	0
Jagannathpur	32900	15290	42773	4928	1	1	3	0
Jamalganj	10510	10250	53570	250	0	1	3	0
Shalla	8142	16053	10547	243	0	2	1	0
Sunamganj Sadar	9336	36330	20167	1268	1	1	4	0
Tahirpur	691	11996	37096	391	0	4	2	0
Total	135002	240916	291768	17036	43	20	19	4

Source: Table produced based on (BBS, 2011b).

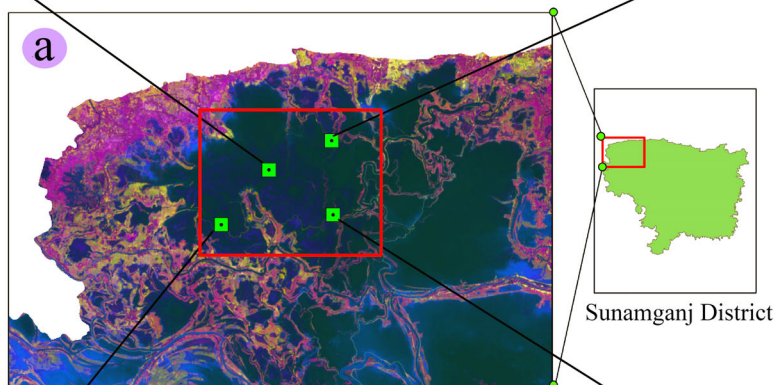


**Image 01**

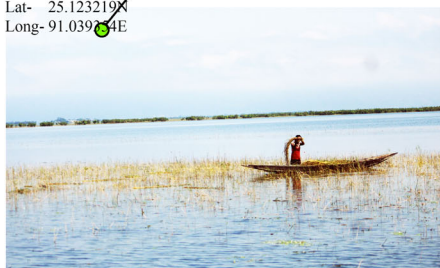
Acquisition date: 13 Nov 2018  
 Location: Tangua Haor, Tahirpur Sunamganj District  
 Lat- 25.149940N  
 Long- 91.057566E

**Image 02**

Acquisition date: 12 Nov 2018  
 Location: Purba Ranga Chara, Tahirpur, Sunamganj District  
 Lat- 25.168153N  
 Long- 91.087382E

**Image 03**

Acquisition date: 13 Nov 2018  
 Location: Moazzampur, Tahirpur, Sunamganj District  
 Lat- 25.123219N  
 Long- 91.03974E

**Image 04**

Acquisition date: 12 Nov 2018  
 Location: Bhabanipur, Tahirpur, Sunamganj District  
 Lat- 25.121490N  
 Long- 91.089222E



Source: Field Survey, November 2018

**Figure 2.** Photographs of flood conditions in the Haor region, Sunamganj District; (a) false-colour composition (FCC) of Haor region.

Source: Photograph taken by Md. Abdul Malak.

embankments that have been inundated by water, thereby forcing people to use boats as their vehicles. Excess rainfall creates surface runoff, and the surface runoff (from Meghalaya hill) causes the waters of the Surma River to swell, which then inundates the riparian zone, as explained below.

### Data sources and analysis

Various satellite data sets were acquired and analysed to meet the aim of this study. This was especially necessary in the case of flash floods whereby there is difficulty in assessing the impact of floods in agricultural and other sectors due to the temporal evolution of inundated areas (Psomiadis *et al.*, 2019). In this study, we acquired several satellite images from every month of each year (including during flooding seasons) to detect perennial waterbodies and month by month temporal extension. A total of 25 multispectral satellite images were used covering the period from November 2016 to October 2017 and November 2018 to October 2019. These comprised 24 images from 24 different months and an additional image of a flooding occurrence in 17 July 2019 (Table 2). In this study, Landsat 8 OLI/TIRS, Sentinel 2 and MODIS multispectral images were used. These were obtained from the US Geological Survey (USGS) website (<https://earthexplorer.usgs.gov/>). The main difficulty encountered in this study was cloud coverage in the monsoon season. Hence, Sentinel 2 and MODIS images were adopted because of the scarcity of cloud-free Landsat 8 OLI/TIRS images in the months of April, May, August and September 2017 and February and June 2019.

**Table 2. Specifications of satellite images used in this study.**

Satellite /Sensor/ Platform	Acquisition date	Path&Row/Tile Number/Granule ID	Spatial Resolution(m)
Landsat 8 OLI	14 November 2016	137/43	30
Landsat 8 OLI	16 December 2016	137/43	30
Landsat 8 OLI	17 January 2017	137/43	30
Landsat 8 OLI	18 February 2017	137/43	30
Landsat 8 OLI	22 March 2017	137/43	30
SENTINEL-2A	12 April 2017	T46RCN8-T46RBN	10
SENTINEL-2A	02 May 2017	T46RCN8-T46RBN	10
Landsat 8 OLI	10 June 2017	137/43	30
Landsat 8 OLI	28 July 2017	137/43	30
MODIS 13Q1	13 August 2017	MOD13Q1.A2017225. h26v06.006.2017250141655	250
MODIS 09Q1	30 September 2017	MOD09Q1.A2017273. h26v06.006.2017282033722	250
Landsat 8 OLI	16 October 2017	137/43	30
Landsat 8 OLI	20November 2018	137/43	30
Landsat 8 OLI	22December 2018	137/43	30
Landsat 8 OLI	23January 2019	137/43	30
SENTINEL-2A	11February 2019	T46RCN8-T46RBN	10
Landsat 8 OLI	28March 2019	137/43	30
Landsat 8 OLI	13April 2019	137/43	30
Landsat 8 OLI	15May2019	137/43	30
SENTINEL-2B	06June2019	T46RCN8-T46RBN	10
Landsat 8 OLI	02July 2019	137/43	30
Landsat 8 OLI	18July 2019	137/43	30
Landsat 8 OLI	19August 2019	137/43	30
Landsat 8 OLI	20September 2019	137/43	30
Landsat 8 OLI	22October 2019	137/43	30
ASTER Global DEM V003VNIR TERRA	13 June 2019	ASTGMTV003_N25E091	30

Source: Table produced by authors.

According to Gao *et al.* (2015), recently launched Sentinel-2 images could be combined with Landsat data for the mapping of crops and waterbodies for various purposes (Gao *et al.*, 2015). Despite some questions of accuracy in delineating flood extent due to the low spatial resolution of MODIS data, such data have been used widely to map vegetation cover as well as flood events due to its high temporal resolution (Memon *et al.*, 2015; Zeng *et al.*, 2020). Although the Landsat 8 OLI/TIRS, Sentinel 2 and MODIS images in this study had spatial resolutions of 30 m, 10 m and 250 m, respectively, a data fusion approach was taken to sort out the spatial resolution mismatch among Landsat 8, Sentinel 2 and MODIS data, following the approach taken elsewhere (Wang *et al.*, 2017; Gao *et al.*, 2015; Gao *et al.*, 2017). Subsequently, Sentinel 2 images were required to create a mosaic that captured the intended study area. To facilitate this, it was necessary to re-project the MODIS data into Universal Traverse Mercator (UTM) Zone 46 N with World Geodetic System 1984 (WGS84) datum and have it clipped to the AOI (area of interest). Although images from July 2017 and August 2019 had a little cloud coverage, the rest were cloud-free. For elevation analysis, ASTER Global DEM V003 (spatial resolution 30 m) was used. The data (scenes or tiles) were retrieved from the NASA geoportal (<https://earthdata.nasa.gov/>) and mosaicked to cover the AOI.

*Multiple water indices analysis and correlation matrix* After obtaining the satellite images, they were clipped with the shapefile of the Sunamganj District. These images were classified by various methods (using multiple water indices) to extract water-related information (Figure 3). Algebraic equations with image bands were applied in several bands viz. Green band, Red band, Near infrared (NIR) band, Shortwave infrared 1 (SWIR1) and Shortwave infrared 2 (SWIR2) band to extract flooded areas. Table S1 illustrates the various formulae of water indices used for waterbody extraction in this study.

Subsequently, all results from the indices were tabulated. As ground data of waterbodies and flooded areas were not available because of the study area's remote geographical location, the rainfall data of the area were used in the correlation matrix to compare against the results from all the indices. All of these results were correlated using Pearson correlation analysis in a correlation matrix. Bivariate correlation tools in SPSS software were used to conduct the Pearson correlation analysis.

*Analysis of annual waterbodies extension* The NDWI method was adopted for this analysis because of its high accuracy rate and maximum matrix value. All 23 images from each month (except two MODIS images) were classified with the NDWI method to extract waterbodies. Those with values greater than zero were considered as water in this classification. NDVI analysis was considered for delineating waterbodies only for MODIS data because of the availability of separate NDVI bands. The permanent water pixels from the dry season (January–March) were considered as perennial waterbodies. Finally, all classified images and classification results were presented in a single graphical format.

*Haor topography and seasonal waterbodies extension analysis* Overall, five topographical flood conditioning factors were analysed using DEM data in Google Earth Engine and ArcGIS 10.8 software (Figure 3); namely:

- a. *Elevation*: Elevation is the most significant factor in flood occurrence because gravitational forces lead water to flow from high elevated regions to low elevated land which creates flooding (Das, 2019; Mojaddadi *et al.*, 2017). The lower elevated region has a higher risk of flooding.



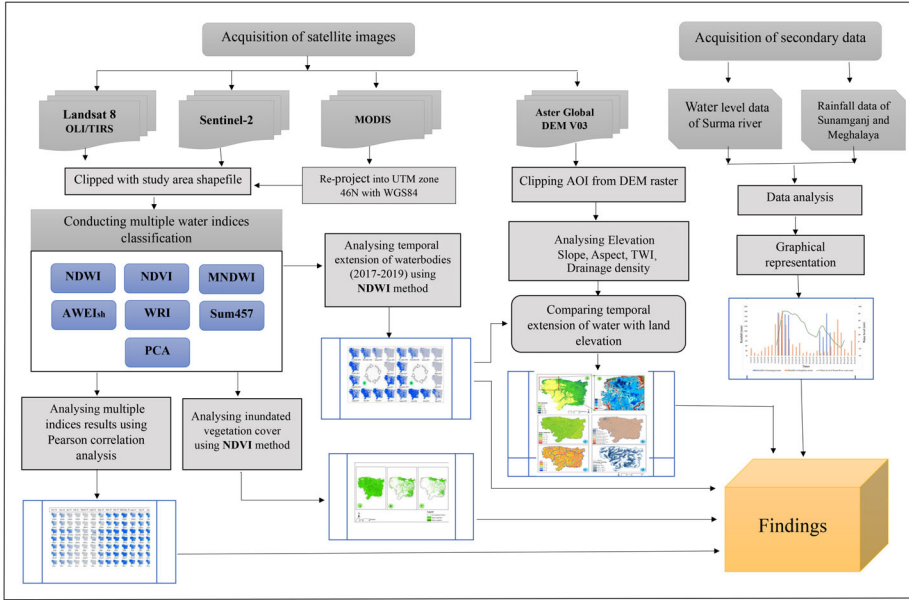


Figure 3. Methodology adopted for the study, AOI = Area of interest, DEM = Digital Elevation Model, UTM = Universal Traverse Mercator.

Source: Figure produced by authors.

- b. *Slope*: Surface runoff, floodwater velocity and water accumulation processes are generally dependent on the topographical slope (Fernandez & Lutz, 2010; Das, 2020). A lower slope represents a higher risk of flooding.
- c. *Aspect*: Aspect is one of the most crucial factors in flooding that helps to identify the flow direction of floodwater (Tehrany & Kumar, 2018).
- d. *Topographic wetness index (TWI)*: The topographic wetness index (TWI) is a term for assessing the tendency of water to accumulate under the influence of gravity at any particular location within a catchment (Shahabi *et al.*, 2020). Moore *et al.* (1991) proposed the following equation to calculate TWI:

$$TWI = \ln(A_s / \tan \beta) \quad (1)$$

Where,  $A_s$  is the specific catchment area ( $m^2 m^{-1}$ ) and  $\beta$  is the slope (in  $^\circ$ ). The higher the TWI value, the higher the risk of flooding.

- e. *Drainage density*: Drainage density is a significant topographical factor of flooding which controls the discharge and flow direction of water (Sajedi-Hosseini *et al.*, 2018). A high drainage density refers to a high density of stream networks per unit of area which is responsible for frequent floodings (Ogden *et al.*, 2011).

Additionally, waterbodies from 6 seasons in 2018–2019 were also assessed and overlapped as different layers over the elevation map in ArcGIS10.4 software. Next, these layers were compared with land elevation to assess the seasonal areal extension of perennial waterbodies.

*Inundated vegetation cover analysis* In this part of the study, the vegetation cover of Sunamganj District was analysed during three major periods: the dry season, the wet season, and the flooding season. Vegetation cover was divided into two categories: sparse and dense. An image from 28 March 2019 was tagged to the dry season while images from 2 July 2019 and 18 July 2019 were associated with the wet and flooding seasons respectively. In Bangladesh, while the month of March distinctly marks the dry season for lack of rain, the month of July is clearly indicative of the wet season due to the onset of the monsoon. Generally, NDVI values that ranged between -1 to 0.19 were considered as non-vegetated features e.g. water, sand, barren land, and settlements. On the contrary NDVI values that fell between 0.2 to 1 were considered as vegetated features (Quader *et al.*, 2021). In order to categorize dense and sparse vegetation more distinctly, we adopted Al-Doski *et al.*'s (2013) value range, whereby values between 0.2–0.4 were considered sparse vegetation and values between 0.4–0.6 were considered dense vegetation.

*Water level data and rainfall data analysis* The water level data of the Surma River and the rainfall data of the Sunamganj District were used in this portion of the study. These data were obtained from the Ministry of Disaster Management and Relief, Government of Bangladesh, through a source known as the Daily Disaster Situation Report (<https://modmr.gov.bd/site/view/situationreport/Daily-Disaster-Situation-Report>). From July to August 2019, daily disaster reports were carefully analysed for flood-related information. Furthermore, the 12-month total rainfall for 2018–2019 in Sunamganj District and daily rainfall data for Meghalaya state were obtained from an international weather news website (i.e. <https://www.worldweatheronline.com>).

Then, water level data and daily rainfall data for the flooding month of July 2019 were tabulated and analysed in MS Excel and SPSS. Finally, the results were presented in a bar chart representing the relationship between rainfall and the water level of the Surma River.

### *The limitations of the study*

There are a few limitations to this work that could be addressed in future research. Firstly, we found that the scarcity of cloud-free images was the main challenge in this study, as almost every part of Bangladesh became cloudy in the monsoon season. Thus, it was not easy to obtain cloud-free images from different platforms during the study period. Consequently, we decided to use high temporal resolution MODIS data for August and September 2017 although these data had low spatial resolutions (250 m). In an ideal situation, more cloud-free images in the monsoon season with high spatial resolution could provide a more accurate measurement of the temporal expansion of waterbodies. Secondly, attaining ground data of the flooded areas was very challenging due to the remote location of the study area. Thus, as an alternative, we used rainfall data in the correlation matrix (Table 3). It would have been more ideal if we had gotten ground data of the flooded area to justify our multiple indices results. Despite these limitations, the findings of this study are still valuable enough to assist disaster management authorities in their flood management, flood forecasting, and agricultural decision-making purposes.

## **Results**

### *Multiple water indices results and correlation matrix*

Figure 4 shows the results that were found from various water extraction methods in a distinct time-frame. The results revealed that MNDWI and AWEIsh methods provided

Table 3. Correlation matrix of classification results from different indices.

	Rainfall	NDWI	NDVI	MNDWI	AWEIsh	WRI	Sum457	PCA
Rainfall	1	0.831	0.817	0.747	0.733	0.770	0.803	0.826
NDWI	0.831	1	0.994	0.929	0.945	0.984	0.967	0.980
NDVI	0.817	0.994	1	0.897	0.917	0.969	0.941	0.966
MNDWI	0.747	0.929	0.897	1	0.990	0.965	0.959	0.924
AWEIsh	0.733	0.945	0.917	0.990	1	0.981	0.967	0.941
WRI	0.770	0.984	0.969	0.965	0.981	1	0.972	0.961
Sum457	0.803	0.967	0.941	0.959	0.967	0.972	1	0.985
PCA	0.826	0.980	0.966	0.924	0.941	0.961	0.985	1

Source: Table produced by authors. Note: All correlation is significant at the 0.01 level.

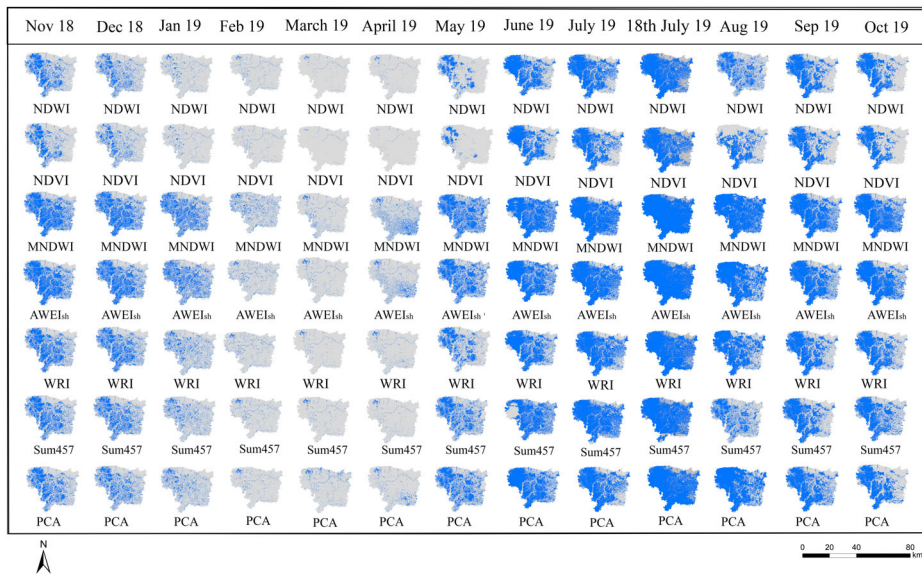


Figure 4. Waterbody extraction by multiple water indices in Sunamganj District. Blue coloured areas represent waterbodies.

Source: Figure produced by authors.

higher results in every time-frame compared to other indices used in this study by detecting numerous non-waterbodies as water pixels. Many of the flood-free zones seemed inundated with MNDWI and AWEI classifications. In contrast, NDVI methods seemed unable to detect shallow water or muddy land; as such, many shallow waterbodies appeared to be dry areas. Evidently, all of the indices showed that the entire district’s waterbodies remained dry from January to April. From all indices, it also cannot be denied that the lion’s portion of the district was inundated by water during the flood of 2019. Subsequently, flooded areas continued to recede in September and October. Despite a few classification errors, the temporal extension of waterbodies was very transparent in all indices.

Table 4 demonstrates the correlation matrix of all indices and the results of different indices found from the Pearson correlation analysis. Compared with rainfall data,

**Table 4. Comparison of floodwater extension between the 2017 flash-flood and the 2019 monsoon flood.**

Month	Temporal extension of waterbodies in Sunamganj District (area in km <sup>2</sup> )	
	Flash-flood 2016-2017	Monsoon flood 2018-2019
November	1651.14	1211.24
December	1260.62	930.59
January	583.53	259.93
February	153.33	150.99
March	36.59	60.2
April	1958.37	83.03
May	2147.95	747.67
June	1969.16	2060.36
July	2154	2783.97
August	1754.43	1946.68
September	1865.18	1876.13
October	2027.10	1580.35

Source: Table produced by authors.

NDWI had the closest correlation value (0.831) among all these indices, where the p-value was 0.01. NDVI, Sum457 and PCA had proximate results to NDWI, 0.817, 0.803 and 0.826, respectively. On the other hand, MNDWI, AWEIsh and WRI provided results (0.747, 0.733 and 0.770) that differed from the rest. Because of high correlation accuracy, it is clear that NDWI is the best method to use for detecting waterbodies in flooded areas; thus, NDWI was used for further analysis in this study.

#### *Comparison of floodwater expansion between the 2017 flash flood and the 2019 monsoon in Sunamganj District*

Sunamganj District is very susceptible to floods because of its geographical location and topography. Specifically, the district has a maximum land surface elevation of less than 10 m.a.s.l comprising partly of the relatively flat low-lying Haor basin, which is essentially a bowl-shaped depression (Kamal *et al.*, 2018; CEGIS, 2012). Flash flood runoff from Meghalaya's upstream hilly catchment often submerges the majority of the Haor region in the Sunamganj District (Kamal *et al.*, 2018). Because of the high accuracy rate in the correlation matrix, NDWI analysis was adopted to assess the perennial waterbodies and annual water circulation of the Sunamganj District.

Figure 5 illustrates the comparison between the temporal expansion of waterbodies in 2016–2017 and 2018–2019. From the NDWI analysis, the Haor basin in both time-frames seemed almost dessicated from the months of January to March. However, the waterbodies in the basin started to expand during the pre-monsoon season of March–April 2017 (Figure 5a) and the monsoon season of June–July 2019 (Figure 5b). Some parts of the Haor region (north-western part of Sunamganj District) were found to be wet the entire year and were considered to be perennial waterbodies. This was especially the case for Tahirpur and Dharamapasha sub-districts which contained the greatest portion of perennial waterbodies that survived in the dry season. Perennial waterbodies in the Sunamganj District in 2017 and 2019 were found to occupy 36.5 km<sup>2</sup> and 60 km<sup>2</sup>, respectively. Some flood-free regions, located in Bishwamvarpur, Chhatak and Dowarabazar sub-districts, could also be identified in Figure 5. Notably, a massive difference was found in the area of waterbodies between

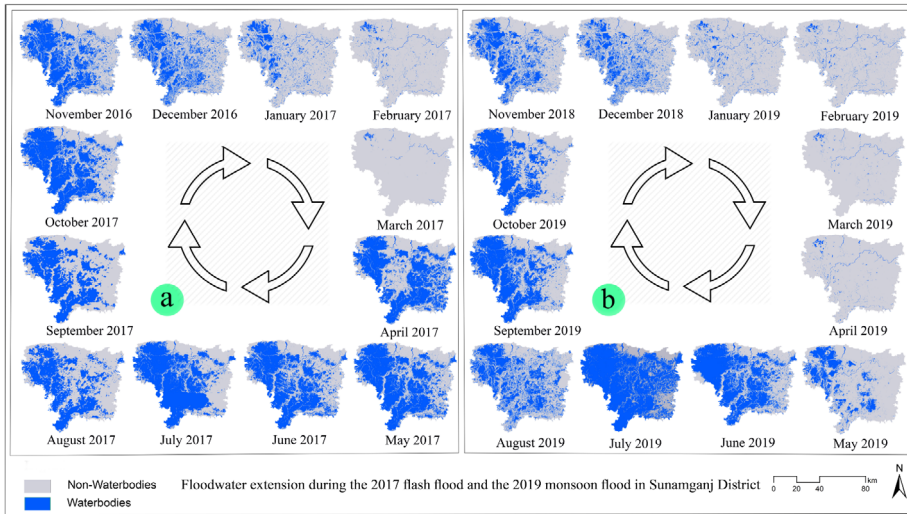


**Figure 5.** Temporal expansion of waterbodies in Sunamganj District; (a) Extension of waterbodies between November 2016 and October 2017, (b) Expansion of waterbodies between November 2018 and October 2019. Source: Figure produced by authors.

April 2017 (1958 km<sup>2</sup>) and April 2019 (83 km<sup>2</sup>). This occurred due to the early 2017 flash flood. In July 2019, perennial waterbodies extended 46 times their perennial area (to almost 2784 km<sup>2</sup>) during the flood. After July–August 2019, water levels started to decline again and return to perennial water levels in January–February in both time-frames.

The basic difference between the pre-monsoon flash flood of 2017 and the monsoon flood of 2019 is found in the temporal extension of waterbodies. A dramatic rise was identified (Table 4) in the 2017 pre-monsoon flash flood where waterbodies expanded very quickly from March to April (extending from 37 km<sup>2</sup> to 1958 km<sup>2</sup>) due to surface runoff from the upper hilly areas. Sudden flooding in the Haor region damaged a vast area of cropping lands during the 2017 flash flood. On 2 May 2017, the inundated area was found to cover a total of 2148 km<sup>2</sup>. In 2019, water extension was detected only after the month of June and the largest inundated area reached was 2784 km<sup>2</sup> on 17 July 2019, more than two and a half months later as compared to the 2017 maximum. The damage from the 2019 monsoon flood was relatively lower than that of the 2017 flash flood. The flooding or water extension in June, July and August of 2019 was to be expected because of the rainfall pattern in the monsoon season in the north-eastern part of Bangladesh. However, the extension of water in March, April, and May of 2017 was unusual and occurred due to excessive early rainfall in the upper basin of the Haor area.

#### *Haor topography and seasonal waterbodies extension analysis*

The low elevation and bowl-shaped topography of the Haor areas are often significant factors that contribute to frequent flooding in the Sunamganj District (Kamal *et al.*, 2018). Figure 6a demonstrates that the Haor basin (north-western part of Sunamganj District) has an average land elevation of less than 2 m.a.s.l. and is very vulnerable to flooding. Almost every year, this region remains inundated because of surface runoff from Meghalaya hills and excessive rainfall. Also, its bowl-shaped flat



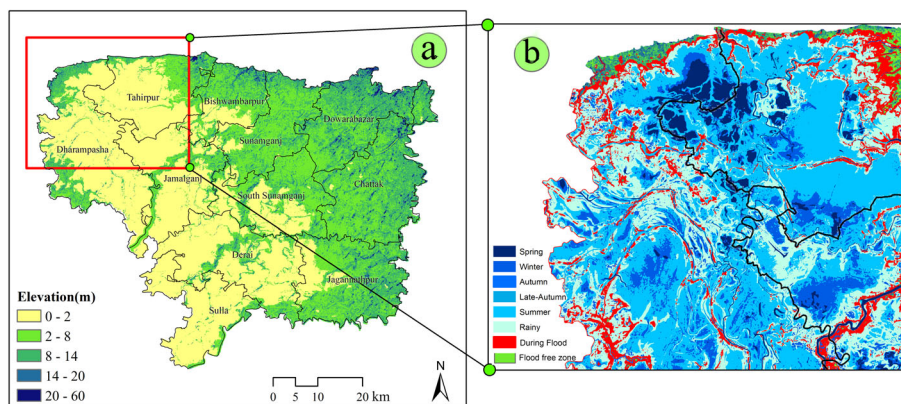


**Figure 6.** Relationship between the land elevation of the Haor region and temporal extension of waterbodies in 2019; (a) Land elevation; (b) Seasonal extension of waterbodies. Red coloured areas in the map represent maximum extension of floodwater during flooding.

Source: Figure produced by authors.

topography makes the Haor zone a water reservoir. There are, however some flood-free areas adjacent to the Meghalaya hill range located in the north-eastern part of this district (Bishwamvarpur sub-district, Chhatak sub-district and Dowaabazar sub-district) with an elevation of around 2060 m.a.s.l.

Figure 6b represents the seasonal temporal extension of waterbodies in the Haor basin. This map confirms the dryness of the spring and winter seasons and shows the gradual extension of waterbodies in this region. During the summer and rainy seasons, the area of waterbodies increased dramatically. In fact, maximum extension occurred in the summer. In the summer, waterbodies spread around eight times the extent that it expanded in the spring season. During the flood of 2019, the waterbodies almost inundated the entire Haor basin. Areas between 8 to 14 m.a.s.l. were also inundated in 2019 by floodwater.

With the exception of a few regions, it can be observed from the slope map of Sunamganj district (Figure 7a), that almost the entire district has a very low slope angle (0–1.1 degrees). This is one of several factors that explain why this region is highly prone to flooding. This susceptibility to flooding also becomes apparent when studying the aspect map of Sunamganj district (Figure 7b) which shows that while a maximum amount of area seems to consist of flat land, no major aspect is found. According, to the Topographic Wetness Index (TWI) map (Figure 7c), the TWI value for the entire region is between 10 to 15 which is at the very high end of the range and another indication of high risk flooding in the region. Further, Figure 7d reveals that the entire study area has a higher drainage density coupled with clustered stream networks. More specifically, Tahirpur and Jamalganj sub-districts, where most of the Haors are located, have higher drainage densities of around 157.1 m/m<sup>2</sup> to 296.6 m/m<sup>2</sup>. It is also worth noting that the length of all stream channel networks in the entire district equates to 1067.84 km.

#### *The effect of flooding on vegetation in the Sunamganj District*

According to NDVI analysis, the dry season recorded almost 2964.1 km<sup>2</sup> and 470.4 km<sup>2</sup> of sparse and dense vegetation cover respectively (Figure 8a). Due to rainfall

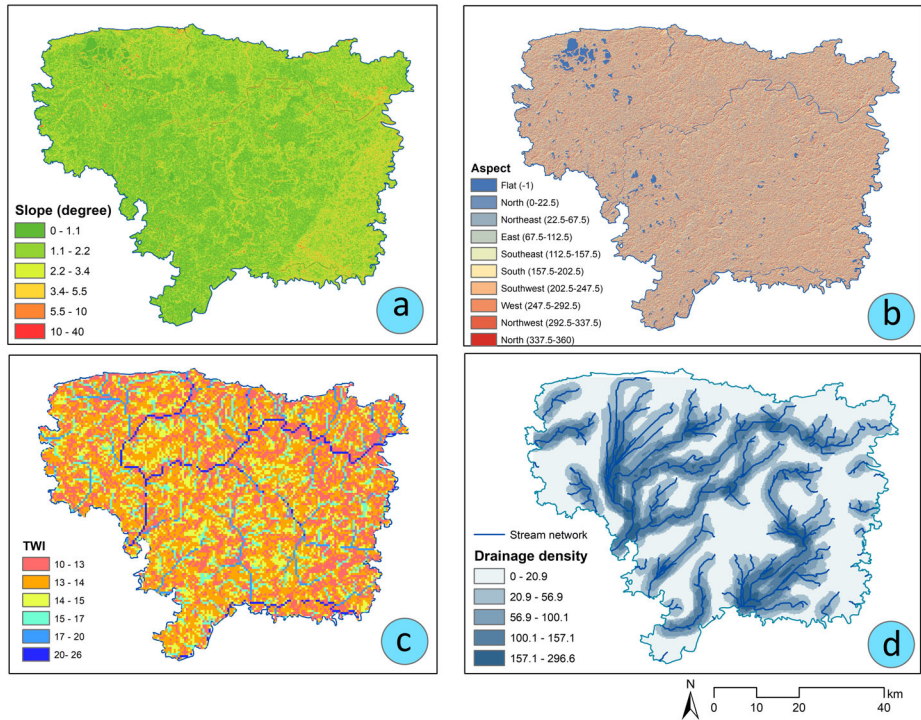


Figure 7. Topographical influences on Haor flooding; (a) Slope (b) Aspect (c) TWI (d) Drainage density. Source: Figure produced by authors.

and surface runoff in the rainy season, agricultural land was submerged by rainwater which accounted for the vegetation cover decline. In the wet season (Figure 8b), while sparse vegetation was found to occupy 563.1 km<sup>2</sup>, dense vegetation was found to occupy only 53.85 km<sup>2</sup>. When the 2019 flood occurred, freshwater mangrove trees like Hijol trees (*Barringtonia acutangular*) were inundated in the Haor region. During the flood (Figure 8c), sparse vegetation was calculated to occupy only 253.97 km<sup>2</sup> while dense vegetation was found to occupy only 1.29 km<sup>2</sup>. NDVI analysis revealed that the monsoon floodwater in 2019 inundated a total of 361.7 km<sup>2</sup> of vegetation cover, including agricultural land where floodwater submerged 309.1 km<sup>2</sup> of sparsely vegetated and 52.6 km<sup>2</sup> of densely vegetated areas. Aside from that, 2401 km<sup>2</sup> of light vegetation and 416.5 km<sup>2</sup> of dense vegetation was submerged due to seasonal extension (dry season→wet season) of waterbodies (Figure 8).

*Rainfall patterns and the water level of the Surma River*

Figure 9 shows that the water level of the Surma River increased because of excessive rainfall that occurred simultaneously in the Sunamganj District and the Meghalaya hilly catchment areas. Very heavy rainfall occurred from 8 July 2019 to 12 July 2019, which raised the water of the Surma River to dangerous levels. Subsequently though, the water level declined slowly over time. The water level of the Surma River rose to 84 cm causing severe flooding (inundating 73.9 per cent of the area) when it overflowed the riverbank in Sunamganj District. On 2 July 2019, the areas inundated in Sunamganj District totalled 2300.5 km<sup>2</sup> and extended up to 2784 km<sup>2</sup> on 17 July

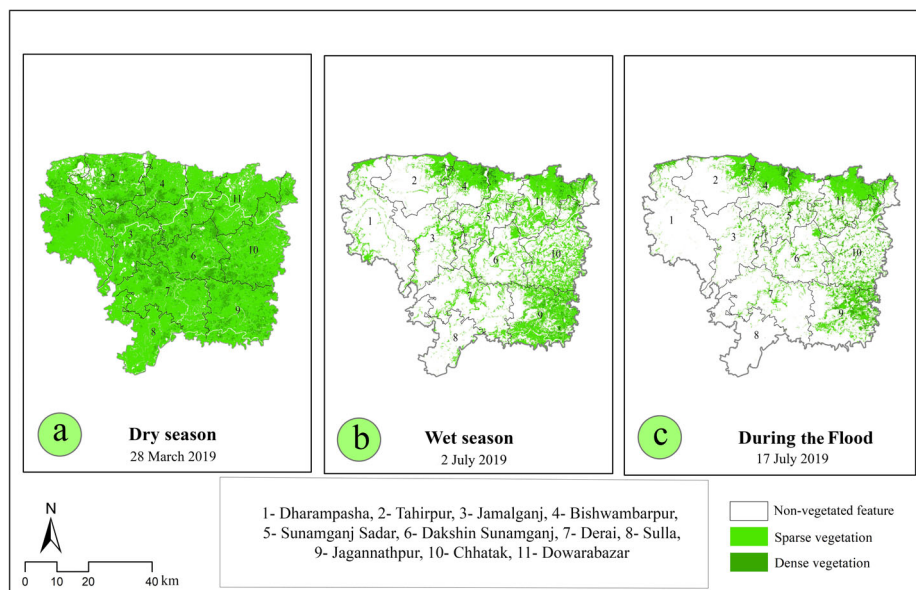


Figure 8. Effects of flooding on vegetation cover in the Sunamganj District. (a) Vegetation cover during the dry season (28 March 2019); (b) Vegetation cover in the wet season (2 July 2019); (c) Vegetation cover during the flood (17 July 2019).

Source: Figure produced by authors.

2019, due to heavy rainfall in Sunamganj District and Meghalaya Hill area. Due to incessant heavy rainfall and the rise of the water level of Surma, the inundated area increased by about 483.5 km<sup>2</sup> during the flood of 2019.

## Discussion

The north-eastern depressed basin provides livelihood opportunities for a significant number of people. Although the land of this low-lying basin is only suitable for single crop cultivation, around 20 per cent of the country's *Boro* rice comes from this region (Kamruzzaman & Shaw, 2018). Additionally, enormous fish stocks and other wetland ecosystem services contribute to both local and national economies. Due to flooding, which is increasing due to global environmental changes, primary livelihood activities of this area are becoming increasingly vulnerable and this has attracted some research and policy attention (Rahman, 2018). Global climate change, in particular, rainfall variation in upstream Meghalaya region of India, is increasing the frequency of pre-monsoon flash floods as well as monsoon floods (Bhattacharjee, 2011). This is threatening the livelihood security of the north-eastern Haor residents (Rahman, 2018). Therefore, close analysis of the flood hazard extension in the north-eastern basin through geo-spatial techniques is necessary to monitor the floodwater extension and promote sustainable livelihood security.

Delineation of the gradual expansion of waterbodies in the Haor region helps to identify the dynamics of flood hazards (Haque *et al.*, 2021). The nature of the extension differs, based on the nature of the flood (i.e., whether caused by flash flooding or monsoon flooding). In 2019, the entire Haor region was dried up from January to April;

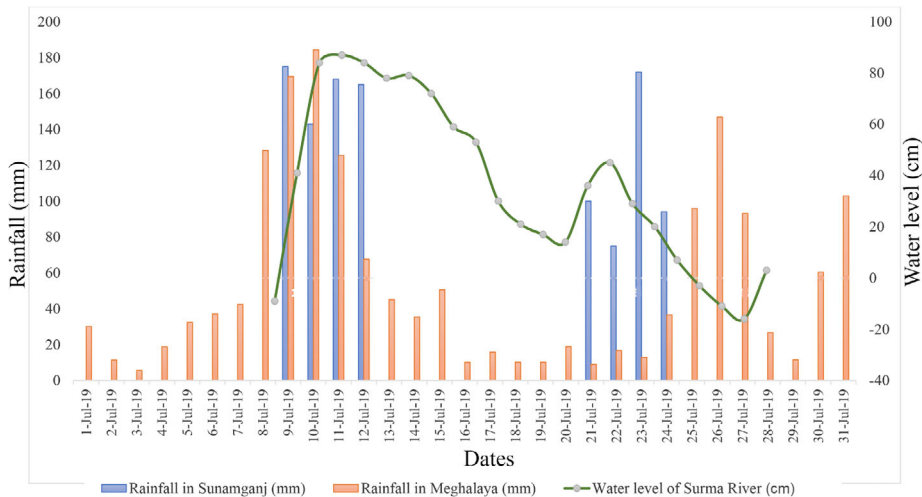


Figure 9. Amount of rainfall in the Sunamganj District and Meghalaya State (India), as well as the water level of Surma River during the flooding season in 2019. Source: Figure produced by authors.

then waterbodies started to increase from May onwards (Figure 4). This happened because stream channels in the entire Sunamganj district (about 1067.84 km, see Figure 7d) dried up from January to April and became significantly flooded in the subsequent monsoon season. Monsoon winds brought rainfall in the Meghalaya catchment and subsequently increased the water level of all stream networks and the Surma River in July 2019 (Figure 9). Flood extension thus depended on the occurrence of rainfall in the upstream and peak discharge of the river water in the case of monsoon flooding (Suman & Bhattacharya, 2015). In terms of water extension, we discovered that pre-monsoon flash floods caused a rapid extension of waterbodies in the research area around April, 2017 (Figure 5). From Figure 5, it is also obvious that waterbodies increased dramatically within a very short period of time from March to April 2017. As *boro* crops (which are considered the staple crops of Haor region) are cultivated during the months of January to May (Mosleh & Hassan, 2014), *boro* cultivation faced severe damage during every pre-monsoon flash flood event because local farmers were unable to collect and save their pre-mature *boro* crops within this short period of time (Kamruzzaman & Shaw, 2018; Abedin & Khatun, 2019). As mentioned earlier, water extension during monsoon floods occur more slowly and later on in the months of June–July over a longer period. By that time, the crops would have already been collected; this translates into a relatively lower crop damage rate during monsoon flooding as compared to during pre-monsoon flash flooding in the Haor region. Optical remote sensing provides ample opportunities to understand the water dynamics of floods, but the result is dependent on the methods used. NDVI, which is a widely used index in such research (Dong *et al.*, 2014; Powell *et al.*, 2014), was found to be less accurate in measuring water extension in the case of monsoon flooding in Haor region whereas the NDWI method achieved maximum accuracy rates.

In this study, NDWI analysis revealed that the perennial waterbodies of Sunamganj District in 2017 and 2019 were 37 km<sup>2</sup> and 60 km<sup>2</sup>, respectively. The largest portion of perennial waterbodies is located in the Tahirpur and Dharamapasha sub-districts. In

the 2017 pre-monsoon period (March–April), these waterbodies increased rapidly in size and inundated a vast proportion of land, including crop land. The inundated area increased 53 times its perennial size within one month (from March to April) in 2017. A study by Aldhshan *et al.* (2019) found that on 26 March 2017, the flooded area was about 4.5 per cent; however, at the beginning of April, flooding occupied around 45 per cent of the area. In 2019, however, our study uncovered that the waterbodies gradually started to extend later on during the monsoon season (June–July). In July 2019, flood water inundated 2784 km<sup>2</sup> of land in total. Within only 16 days (2 July 2019 to 18 July 2019), floodwater extended over 484 km<sup>2</sup> in area.

Two primary reasons were found to be behind frequent flooding in the Sunamganj District and especially in Haor areas. First, excessive rainfall in Sunamganj District and the upper hill catchment of Meghalaya raises the water level of the Surma River (Figure 9) which then overflows the riverbank (Bhattacharjee, 2011). Secondly, this is exacerbated by the bowl-shaped low topography of the Haor region. Indeed, previous results have revealed the average land elevation of the Haor region to be about 1–2 m.a.s.l (CEGIS, 2012). Moreover, the elevation of surrounding highlands of the Haor basin measures 8–14 m.a.s.l., which places it at a much higher level than the depressed basin (Figure 6a), so that water (rainwater and surface runoff from the Meghalaya hills) flows and assembles in the depression, creating flooding conditions. The study also found that the Haor region in Sunamganj District remained dry with the exception of some deep beels in the winter–spring season; then the water level dramatically rises in the summer and monsoon seasons due to inclement rains. Similarly, CEGIS (2012) found the maximum land surface elevation of the Haor wetlands to be less than 10 m. a.s.l. during the monsoon season; these lands were inundated with floodwater for 7–8 months to a typical depth of 0–5 m.a.s.l. In another study conducted in 1988, Islam and Sado (2000) used NOAA digital elevation data to estimate the combined flooded area in Bangladesh between 18 and 24 September and 8 October 1988 and found that it fell between the range of 47 per cent to 50 per cent, while 68 per cent of the flooded area lay between 0 and 12 m.a.s.l. in elevation. It is quite clear from the above findings that low elevation is a significant factor contributing to frequent flooding in the Haor region. There are, however, some flood-free regions adjacent to the Meghalaya hill range in the north-eastern part of this district (Bishwamvarpur, Chhatak and Dowa-rabazar sub-districts). These areas were classified as highland areas (20 to 60 m.a.s.l.) that remained dry during the flooding seasons. Aside from low topography, low slope angles, flat aspect, high TWI and high drainage density are additional factors responsible for frequent flooding in the north-eastern depressed basin of Bangladesh (Figure 7). Furthermore, in mid-July 2019, rainfall caused the Surma River's water level to rise to 84 cm, inundating 73.9 per cent of the total area of Sunamganj District, including a vast portion of agricultural land. Notably, Hoque *et al.* (2011) also found inundated areas to be related to the highest rainfall and peak water levels. Hence, high annual rainfall also accounts for frequent flash flooding in the low-lying Haor (wet-land) region of north-eastern Bangladesh, including Sunamganj District (Kamal *et al.*, 2018; Humanitarian Response, 2017).

In relation to flood impact on the vegetation of Sunamganj District, the data showed that almost 361.7 km<sup>2</sup> of vegetation cover (including agricultural land) was inundated by floodwater in 2019. Part of the inundated land comprised 309.1 km<sup>2</sup> of sparse vegetation and 52.6 km<sup>2</sup> of dense vegetation (Figure 8). According to Hossain *et al.* (2017), available land declined from 47.86 per cent to 14.22 per cent. Almost 33.64 per cent of agricultural land was inundated in the flash flood of April 2017. Ahmed *et al.* (2017)



found that the crops of Sunamganj District did not survive floodwater and was significantly damaged. While NDVI-values were close to 0.4 in the first imaging date after the flooding event (7 April 2017), they were close to zero or negative in the following imaging dates (23 April 2017). The fall in NDVI values indicated that *boro* crops that initially survived were ultimately submerged and damaged by floodwater. The most affected district was Sunamganj District, whereby about 65 per cent of cultivated *boro* crops were damaged in 2017. As the Haor region vastly contributes to the national economy, flood impacts could potentially affect an estimated annual production of 5.25 million MT of rice (Humanitarian Response, 2017). In a study conducted by Uddin *et al.* (2019) in the Sylhet and Rangpur divisions, the authors estimated agricultural land damage caused by the 2017 floods to be 1.51 per cent in April, 3.46 per cent in June and 5.30 per cent in August. Evidently, the country's GDP suffers from vast losses due to floods almost every year. This affects not just GDP, but individual livelihoods and nutrition. Scarcity increases the price of rice, causing a reduction in its affordability to the general population. It also places pressure on governments to subsidise distribution of what remains after flooding.

## Conclusion

The aim of this study is to (i) assess the temporal and spatial dynamics of the maximum flood extent during the pre-monsoon flash flood of 2017 and monsoon flood of 2019 and (ii) identify the perennial waterbodies in Sunamganj District using geospatial techniques. Various indices have been used to assess the flooded areas. We found that NDWI performs very well compared to other methods; notably, the correlation matrix revealed that NDWI, NDVI, Sum457 and PCA had almost similar correlation values, respectively: 0.831, 0.817, and 0.803 and 0.826 when compared with the rainfall data of Sunamganj District. On the other hand, correlation values from MNDWI, AWEIsh, and WRI (0.747, 0.733, and 0.770, respectively) differed from the other indices. NDWI analysis revealed that perennial waterbodies in 2017 and 2019 were assessed respectively to be 37 km<sup>2</sup> and 60 km<sup>2</sup> in Sunamganj District. In the 2017 pre-monsoon flash flood, waterbodies noticeably increased from March to April. However, in July 2019, monsoon flood waterbodies started to extend after May and flooded an area of 2784 km<sup>2</sup>. A Digital Elevation Model map was also analysed to determine the Haor basin's mean altitude which was found to be below 2 m.a.s.l. In winter and spring, the Haor basin remained dry; but at the beginning of summer, waterbodies increased dramatically due to rainfall and surface runoff from the Meghalaya hill range. NDVI analysis revealed that 361.7 km<sup>2</sup> of vegetation cover was inundated by floodwater, including agricultural land in the 2019 monsoon flood. During that flood, the Surma River's water level rose to 84 cm which caused flooding of almost 73.9 per cent of Sunamganj District.

This study has uncovered the water extension processes of pre-monsoon flash flooding and monsoon flooding, which we hope could help the government and authorities concerned with flood monitoring, mapping and management. Moreover, this study's findings could be beneficial for agronomists and local farmers in decision-making for crops cultivation in the Haor region by demarcating flooded zones. The findings of this research could also benefit the disaster management authorities of flood-prone countries to predict and manage impending flood hazards. Furthermore, we hope that the visualization of floodwater extension and Haor topography in this paper would help readers to better understand how floodwater gradually extends in such areas.

## Acknowledgements

We would like to acknowledge the Ministry of Science and Technology, Bangladesh for providing National Science and Technology (NST) Fellowship funding as well as USGS and NASA for providing us with free access to satellite images. The Department of Geography and Environment, Jagannath University is hereby acknowledged for providing us with logistic support during the research. We extend our gratitude to Elaine Newby for improving the language of the manuscript.

## References

- Abedin J, Khatun H (2019) Impacts of flash flood on livelihood and adaptation strategies of the Haor inhabitants: a study in Tanguar Haor of Sunamganj, Bangladesh. *The Dhaka University Journal of Earth and Environmental Sciences* **8** (1), 41–51.
- Acharya TD, Subedi A, Lee DH (2018) Evaluation of water indices for surface water extraction in a Landsat 8 scene of Nepal. *Sensors* **18** (8), 2580. Available at: <https://doi.org/10.3390/s18082580>.
- Adnan MSG, Abdullah AYM, Dewan A, Hall J W (2020) The effects of changing land use and flood hazard on poverty in coastal Bangladesh. *Land Use Policy* **99**, 104868. Available at: <https://doi.org/10.1016/j.landusepol.2020.104868>.
- Adnan MSG, Haque A, Hall JW (2019) Have coastal embankments reduced flooding in Bangladesh? *Science of the Total Environment* **682**, 405–16.
- Ahmed F, Moors E, Khan MSA, Warner J, Van Scheltinga CT (2018) Tipping points in adaptation to urban flooding under climate change and urban growth: the case of the Dhaka megacity. *Land Use Policy* **79**, 496–506.
- Ahmed MR, Rahaman KR, Kok A, Hassan QK (2017) Remote sensing-based quantification of the impact of flash flooding on the rice production: a case study over North-eastern Bangladesh. *Sensors* **17** (10), 2347. Available at: <https://doi.org/10.3390/s17102347>.
- Al-Doski J, Mansor SB, Shafri HZM (2013) NDVI differencing and post-classification to detect vegetation changes in Halabja City, Iraq. *IOSR Journal of Applied Geology and Geophysics* **1** (2), 1–10.
- Aldhshan SR, Mohammed OZ, Shafri HM (2019) Flash flood area mapping using sentinel-1 SAR data: a case study of eight upazilas in Sunamganj District, Bangladesh. *IOP Conference Series: Earth and Environmental Science* **357** (1), 012034. Available at: <https://doi.org/10.1088/1755-1315/357/1/012034>.
- Al Jazeera (2019) Worst floods in years submerge Bangladesh villages. 17 July. Available at: <https://www.aljazeera.com/news/2019/07/worst-floods-years-submerge-bangladesh-villages-190719083053518.html> (accessed 6 November 2019).
- Baishakhy SD, Islam MA (2018) Adaptive behaviour of rice farmers against climate change induced flash flood in Haor areas: emphasizing their socioeconomic traits. *Asian Journal of Agricultural Extension, Economics & Sociology* **35**, 83–94.
- Banerjee L (2007) Effect of flood on agricultural wages in Bangladesh: an empirical analysis. *World Development* **35** (11), 1989–2009.
- Basher MA, Stiller-Reeve MA, Islam AS, Bremer S (2018) Assessing climatic trends of extreme rainfall indices over northeast Bangladesh. *Theoretical and Applied Climatology* **134** (1), 441–52.
- BBC News (2019) Monsoon floods kill dozens and displace millions in India. 18 July. Available at: <https://www.bbc.com/news/world-asia-india-49028155> (accessed 7 November 2019).
- BBS (2011a) Population and housing census, Sunamganj. Available at: [http://203.112.218.65:8008/WebTestApplication/userfiles/Image/PopCen2011/COMMUNITY\\_Sunamganj.pdf](http://203.112.218.65:8008/WebTestApplication/userfiles/Image/PopCen2011/COMMUNITY_Sunamganj.pdf) (accessed 9 November 2019).
- BBS (2011b) District Statistics 2011 Sunamganj. Available at: <http://203.112.218.65:8008/WebTestApplication/userfiles/Image/District%20Statistics/Sunamganj.pdf> (accessed 4 March 2021).
- Benson C, Clay E (2002) Bangladesh: disasters and public finance. Disaster Risk Management Working Paper Series 5. World Bank, Washington, DC.

- Bhattacharjee, S (2011) Uncertainties of flash flood in context of climate change in Sunamganj district, Bangladesh. In Beighley RE II, Killgore MW (eds) *World Environmental and Water Resources Congress 2011: Bearing Knowledge for Sustainability*, 4564–71. ASCE, Reston.
- Bhuiyan MJAN, Dutta D (2012) Analysis of flood vulnerability and assessment of the impacts in coastal zones of Bangladesh due to potential sea-level rise. *Natural Hazards* **61** (2), 729–43.
- Centre for Environmental and Geographic Information Service (CEGIS) (2012) Master Plan of Haor Areas. Haor and Wetland Development Board, Ministry of Water Resources, Bangladesh. Available at: <http://fpd-bd.com/wp-content/uploads/2015/07/Master-plan-of-haor-areas.pdf> (accessed 10 November 2019).
- Daily Star (2019a) Heavy rains to cause flash floods again. Staff correspondent, 9 August. Available at: <https://www.thedailystar.net/backpage/heavy-rains-in-bangladesh-cause-flash-floods-again-1783864> (accessed 6 November 2019).
- Daily Star (2019b) 13 lakh affected in north, hill dists. Star report, 14 July. Available at: <https://www.thedailystar.net/frontpage/13-lakh-marooned-north-hill-dists-in-bangladesh-1771009> (accessed 7 November 2019).
- Das MK, Saiful IA, Jamal Uddin KM, Samarendra, K (2017) Numerical simulation of flash-flood-producing heavy rainfall of 16 April 2016 in NE regions of Bangladesh. *Vayu Mandal* **43** (2), 97–108.
- Das S (2019) Geospatial mapping of flood susceptibility and hydro-geomorphic response to the floods in Ulhas basin, India. *Remote Sensing Applications: Society and Environment* **14**, 60–74.
- Das S (2020) Flood susceptibility mapping of the Western Ghat coastal belt using multi-source geospatial data and analytical hierarchy process (AHP). *Remote Sensing Applications: Society and Environment* **20**, 100379. Available at: <https://doi.org/10.1016/j.rsase.2020.100379>.
- Dewan A (2013) *Floods in a Megacity: Geospatial Techniques in Assessing Hazards, Risk and Vulnerability*. Springer, Dordrecht.
- Dong Z, Wang Z, Liu D *et al.* (2014) Mapping wetland areas using Landsat-derived NDVI and LSWI: a case study of West Songnen plain, Northeast China. *Journal of the Indian Society of Remote Sensing* **42** (3), 569–76.
- Fernandez DS, Lutz MA, (2010) Urban flood hazard zoning in Tucuman Province, Argentina, using GIS and multicriteria decision analysis. *Engineering Geology* **111** (1–4), 90–8.
- Gao F, Anderson MC, Zhang X *et al.* (2017) Toward mapping crop progress at field scales through fusion of Landsat and MODIS imagery. *Remote Sensing of Environment* **188**, 9–25.
- Gao F, Hilker T, Zhu X *et al.* (2015) Fusing Landsat and MODIS data for vegetation monitoring. *IEEE Geoscience and Remote Sensing Magazine* **3** (3), 47–60.
- Haibo Y, Zongmin W, Hongling Z, Yu G (2011) Waterbody extraction methods study based on RS and GIS. *Procedia Environmental Sciences* **10**, 2619–24.
- Haque MI, Basak R (2017) Land cover change detection using GIS and remote sensing techniques: a spatio-temporal study on Tanguar Haor, Sunamganj, Bangladesh. *Egyptian Journal of Remote Sensing and Space Science* **20** (2), 251–63.
- Haque MN, Siddika S, Sresto MA, Saroar MM, Shabab KR (2021) Geo-spatial analysis for flash flood susceptibility mapping in the North-East Haor (wetland) region in Bangladesh. *Earth Systems and Environment* **5**, 365–84.
- Hoque MAA, Tasfia S, Ahmed N, Pradhan B (2019) Assessing spatial flood vulnerability at Kalapara Upazila in Bangladesh using an analytic hierarchy process. *Sensors* **19** (6), 1302. Available at: [10.3390/s19061302](https://doi.org/10.3390/s19061302).
- Hoque R, Nakayama D, Matsuyama H, Matsumoto J (2011) Flood monitoring, mapping and assessing capabilities using RADARSAT remote sensing, GIS and ground data for Bangladesh. *Natural Hazards* **57** (2), 525–48.
- Hossain MS, Nayeem A, Majumder AK (2017) Impact of flash flood on agriculture land in Tanguar Haor Basin. *International Journal of Research in Environmental Science* **3** (4), 42–5.
- Humanitarian Response (2017) Floods in Northeast (Haor) areas of Bangladesh, April-May 2017. Assessment report. Government of Bangladesh, Dhaka. Available at: <https://www.humanitarianresponse.info/sites/www.humanitarianresponse.info/files/2019/07/Bangladesh-Floods-in-Northeast-%28Haor%29-areas.pdf> (accessed 14 June 2020).

- Islam AS, Bala SK, Haque MA (2010) Flood inundation map of Bangladesh using MODIS time-series images. *Journal of Flood Risk Management* **3** (3), 210–22.
- Islam MM, Sado K (2000) Flood hazard assessment in Bangladesh using NOAA AVHRR data with geographical information system. *Hydrological Processes* **14** (3), 605–20.
- Jeyaseelan AT (2004) Drought and floods assessment and monitoring using remote sensing and GIS. In Sivkumar MVK, Roy PS, Harmsen K, Saha SK (eds) *Satellite Remote Sensing and GIS Applications in Agricultural Meteorology*, 291–313. World Meteorological Organization, Geneva.
- Kamal AM, Shamsudduha M, Ahmed B *et al.* (2018) Resilience to flash floods in wetland communities of north-eastern Bangladesh. *International Journal of Disaster Risk Reduction* **31**, 478–88.
- Kamruzzaman M, Shaw R (2018) Flood and sustainable agriculture in the Haor Basin of Bangladesh: a review paper. *Universal Journal of Agricultural Research* **6** (1), 40–9.
- Karim MF, Mimura N (2008) Impacts of climate change and sea-level rise on cyclonic storm surge floods in Bangladesh. *Global Environmental Change* **18** (3), 490–500.
- Kwak Yj (2017) Nationwide flood monitoring for disaster risk reduction using multiple satellite data. *ISPRS International Journal of Geo-Information* **6** (7), 203. Available at: <https://doi.org/10.3390/ijgi6070203>.
- Malik S, Pal SC, Chowdhuri I, Chakraborty R, Roy P, Das, B (2020) Prediction of highly flood prone areas by GIS based heuristic and statistical model in a monsoon dominated region of Bengal Basin. *Remote Sensing Applications: Society and Environment* **19**, 100343. Available at: <https://doi.org/10.1016/j.rsase.2020.100343>.
- Memon AA, Muhammad S, Rahman S, Haq M (2015) Flood monitoring and damage assessment using water indices: a case study of Pakistan flood-2012. *Egyptian Journal of Remote Sensing and Space Science* **18** (1), 99–106.
- Ministry of Disaster Management and Relief (2019) *Daily Disaster Situation Report*. Available at: <http://modmr.gov.bd/site/view/situationreport/Daily-Situation-Report> (accessed 6 September 2019).
- Mirza MMQ (2002) Global warming and changes in the probability of occurrence of floods in Bangladesh and implications. *Global Environmental Change* **12** (2), 127–38.
- Mojaddadi H, Pradhan B, Nampak H, Ahmad N, Ghazali AHB (2017) Ensemble machine learning-based geospatial approach for flood risk assessment using multisensory remote-sensing data and GIS. *Geomatics, Natural Hazards and Risk* **8**, 1080–102.
- Moore ID, Grayson R, Ladson A (1991) Digital terrain modelling: a review of hydrological, geomorphological, and biological applications. *Hydrological Processes* **5** (1), 3–30.
- Mosleh MK, Hassan QK (2014) Development of a remote sensing-based “Boro” rice mapping system. *Remote Sensing* **6** (3), 1938–53.
- Ogden FL, Raj Pradhan N, Downer CW, Zahner JA (2011) Relative importance of impervious area, drainage density, width function, and subsurface storm drainage on flood runoff from an urbanized catchment. *Water Resources Research* **47** (12). Available at: [10.1029/2011WR010550](https://doi.org/10.1029/2011WR010550).
- Powell SJ, Jakeman A, Croke B (2014) Can NDVI response indicate the effective flood extent in macrophyte dominated floodplain wetlands? *Ecological Indicators* **45**, 486–93.
- Profeti G, Macintosh H (1997) Flood management through Landsat TM and ERS SAR data: a case study. *Hydrological Processes* **11** (10), 1397–408.
- Psomiadis E, Soulis KX, Zoka M, Dercas N (2019) Synergistic approach of remote sensing and GIS techniques for flashflood monitoring and damage assessment in Thessaly plain area, Greece. *Water* **11** (3), 448. Available at: <https://doi.org/10.3390/w11030448>.
- Quader MA, Dey H, Malak MA, Sajib AM (2021) Rohingya refugee flooding and changes of the physical and social landscape in Ukhiya, Bangladesh. *Environment, Development and Sustainability* **23**, 4634–58.
- Rahman HT (2018) *Livelihood Vulnerability to Climatic Stresses: A Study of the Northeastern Flood Plain Communities of Bangladesh* (PhD thesis). Department of Natural Resource Sciences, McGill University.
- Rahman MM, Hossain MA, Bhattacharya AK (2007) Flood management in the flood plain of Bangladesh. Paper presented at the International Conference on Civil Engineering in the New Millennium: Opportunities and Challenges (CENM), 11–14 January, Kolkata, India.

- Rayhan MI (2010) Assessing poverty, risk and vulnerability: a study on flooded households in rural Bangladesh. *Journal of Flood Risk Management* **3** (1), 18–24.
- Roy B, Islam AS, Islam GT *et al.* (2019) Frequency analysis of flash floods for establishing new danger levels for the rivers in the northeast Haor region of Bangladesh. *Journal of Hydrologic Engineering* **24** (4), 05019004. Available at: [https://doi.org/10.1061/\(ASCE\)HE.1943-5584.0001760](https://doi.org/10.1061/(ASCE)HE.1943-5584.0001760).
- Roy SK, Sarker SC (2016) Integration of remote sensing data and GIS tools for accurate mapping of flooded area of Kurigram, Bangladesh. *Journal of Geographic Information System* **8** (2), 184–92.
- Sajedi-Hosseini F, Choubin B, Solaimani K, Cerdà A, Kaviani A (2018) Spatial prediction of soil erosion susceptibility using a fuzzy analytical network process: application of the fuzzy decision making trial and evaluation laboratory approach. *Land Degradation & Development* **29** (9), 3092–3103.
- Salaudin M, Islam AKMS (2011) Identification of land cover changes of the Haor area of Bangladesh using Modis Images. In *Proceedings of the 3rd International Conference on Water & Flood Management (ICWFM-2011)*. Institute of Water and Flood Management, BUET, Dhaka.
- Shahabi H, Shirzadi A, Ghaderi K *et al.* (2020) Flood detection and susceptibility mapping using sentinel-1 remote sensing data and a machine learning approach: hybrid intelligence of bagging ensemble based on k-nearest neighbor classifier. *Remote Sensing* **12** (2), 266. Available at: <https://doi.org/10.3390/rs12020266>.
- Suman A, Bhattacharya B (2015) Flood characterisation of the Haor region of Bangladesh using flood index. *Hydrology Research* **46** (5), 824–35.
- Tehrany MS, Kumar L (2018) The application of a Dempster–Shafer-based evidential belief function in flood susceptibility mapping and comparison with frequency ratio and logistic regression methods. *Environmental Earth Sciences* **77** (13), 490. Available at: <https://doi.org/10.1007/s12665-018-7667-0>.
- Tv B, Kn N (2019) A comparative study of spectral indices for surface water delineation using Landsat 8 Images. Paper presented at the 2019 International Conference on Data Science and Communication (IconDSC), 1–2 March, Bangalore, India.
- Uddin K, Matin MA, Meyer FJ (2019) Operational flood mapping using multi-temporal sentinel-1 SAR images: a case study from Bangladesh. *Remote Sensing* **11** (13), 1581. Available at: [10.3390/rs11131581](https://doi.org/10.3390/rs11131581).
- Wang Q, Blackburn GA, Onojeghuo AO (2017) Fusion of Landsat 8 OLI and Sentinel-2 MSI data. *IEEE Transactions on Geoscience and Remote Sensing* **55** (7), 3885–99.
- Zeng L, Wardlow BD, Xiang D, Hu S, Li D (2020) A review of vegetation phenological metrics extraction using time-series, multispectral satellite data. *Remote Sensing of Environment* **237**, 111511. Available at: <https://doi.org/10.1016/j.rse.2019.111511>.

## Supporting Information

Additional supporting information may be found online in the Supporting Information section at the end of the article.

**Table S1.** Indices used in the assessment of flood hazards with their descriptions, algorithm and threshold values.